International Journal of Environmental Sciences
ISSN: 2229-7359
Vol. 11 No. 16s, 2025
https://www.theaspd.com/ijes.php

Synthesis, Characterization, Biological Activity And Molecular Docking Studies Of 1,2,4-Triazole Linked Quinoline Derivatives

G. Sreelatha[1], P. Sateesh Kumar[2], E. Balraju[3] and Aliya Begum[4*]

[1,3]Department of Chemistry, Osmania University, Hyderabad, Telangana State, India
[2]University PG College (OU), Siddipet, Telangana State, India
[4*]Department of Chemistry, Telangana Mahila Viswa Vidyalayam, Hyderabad, Telangana, India.

***Corresponding author**: Aliya Begum
*Email: draliyaou@gmail.com

ABSTRACT

With the use of cyclization and Schiff's base reactions, a new group of 1,2,4-triazole-linked quinoline derivatives (3a – 3j) was effectively synthesized with yields ranging from moderate to excellent. The potential anticancer, antibacterial, and anthelmintic medicinal properties of these compounds were subsequently studied through molecular docking studies. The MTT analysis method was employed to evaluate anticancer activity, and the most efficient derivatives were compounds ***I-3b****,* ***I-3f****, and* ***I-3j****, with IC50 values of* ***23.46±0.001****,* ***20.02±0.013****, and* ***25.76±0.016****μg/mL exhibiting good activity, according to the data. In comparison to streptomycin, antibacterial studies against both Gram-positive and Gram-negative bacteria showed significant actions. Furthermore, they showed anthelmintic properties when tested against albendazole. Molecular docking research revealed that the binding energies of all of the substances ranged from* ***-9.1 to -10.8 Kcal/mol.***

KEYWORDS: *Substituted Quinoline, Doxorubicin, Anticancer, Antibacterial and Anthelmintic activities, MTT assay.*

1. INTRODUCTION

A logical and promising avenue in contemporary medicinal chemistry is the design of novel drug-like small compounds based on pharmacologically active scaffolds. Integrating physiologically active pharmacophores has generated a number of compounds that medicinal chemists have used to develop new therapeutic medicines with an abundance of pharmacological actions. Numerous biological and pharmacological actions can be observed by the synthetic compounds which contain the quinoline substructure as a pharmacophore[1-3]. It is believed that an important function for quinoline as a structural motif among biologically active molecules and for the combinatorial assembly of heterocyclic scaffolds. Quinoline is a heterocyclic aromatic molecule composed of oxygen and nitrogen atoms that are abundant in electrons. Anticancer, anti-inflammatory, analgesic, muscle relaxant, sedative, anti-tubercular, diuretic, antibacterial, anticonvulsant, anti-allergic, anti-malarial, antiviral, antioxidant, and central nervous system depressant characteristics have been observed for compounds that include a quinoline ring residue[4-7].

Resistant to multiple drugs bacteria, frequently referred to as MDR bacteria, have become more common, and a number of harmful organisms have developed resistance to at least one class of antibiotics that are presently in use[8-9]. Fluoroquinolones are a particularly common name for quinolones because of their inclusion of fluorine in their chemical structure. Quinolones execute their effects by causing chromosomal damage in bacteria[10]. Nevertheless, the current quinolones have drawbacks, which includes their poor efficacy against a number of vital Gram-positive bacteria. The nitrogen-containing heterocyclic a compound quinazolinone (QNZ) is an element of about 200 naturally generated alkaloids that have been isolated from different types of microbes, plants, and animals[11]. In view of their biopharmaceutical characteristics, anticancer, diuretic, anti-inflammatory, anticonvulsant, and antihypertensive characteristics, these compounds have been thoroughly investigated by connecting many kinds of beneficial groups to the quinazoline moiety. Numerous investigations into quinazolinone substituents have been performed during the last decades; these publications explored multiple aspects of synthesis, characterisation, biomedical treatment, and QNZ loading into diverse nanoparticle forms, and integration of nanoparticles in QNZ manufacturing processes[12]. As an example, magnetic

nanoparticles are being used to sustain the catalyst factor in multicomponent reactions, promote their reactivity and reusability, and keep the catalyst from migrating from the reaction the environment.

2. EXPERIMENTAL SECTION

2. 1. Material and Method

All reagents and solvents were purified and dried by standard techniques. S.D. Fine Chem. Ltd., Sigma Hi-media, Rolex, Reachem, Aldrich, and Rolex supplied the AR and LR grade chemicals and reagents used in the present investigation. A Veergo digital melting point analyzer was implemented to test the uncorrected melting points in open capillary tubes. Applying ethyl acetate and n-hexane (1:2), TLC has been carried out on 0.25 mm thick silica gel GF254 coated plates. The BRUKER AVANCE II 400MHz NMR Spectrometer instrument was put to use to record the 1HNMR spectra of the made compounds in deuterated DMSO, using TMS acting as the internal standard. The Perkin Elmer FTIR spectrophotometer had been utilised to record the IR spectra using KBr pellets. Dimethyl sulfoxide (DMSO) has been employed as a solvent in the LC-MSD Tranp-SL2010A SHIMADZU for capturing mass spectra.

2.2. General Synthetic Procedure:

The specified work is based on cyclization and Schiff's base reactions which involve reaction between TCH with benzoic acid, then it reacts with quinoline-3-carbaldehyde to form get title (3a-3j) derivatives.

Step-I: Synthesis of 4-amino-5-phenyl-3-thiol-1,2,4-Triazole (1): A round-bottom flask has been filled with a solution of thiocarbohydrazide (0.015 mol) and benzoic acid (0.01 mol). For five minutes at a time, the mixture was heated in a sand bath. Employing TLC, the reaction's completeness was determined. Following cooling, the addition of frigid water to the reaction mixture, the resultant precipitate was filtered and treated a water wash.. Utilizing ethanol, the product was recrystallized.

Step-II: Synthesis of 4-{(2-chloro-6-bromo quinolin-3yl)methylidene)amino}-5-phenyl-4H-1,2,4-triazole-3-thiol (3a-3j): Solution of appropriate 4-amino-5-phenyl-3-thiol-1,2,4-Triazole (Hybrid Azine Derivatives Encyclopedia Hybrid Azine Derivatives) (1) (0.01mol) and substituted quinoline-3-carbaldehyde (2) (0.01mol) were added. In order to bring the pH down to about 4.5, add between two and three drops of glacial acetic acid or coper chloride (0.5 mmol. Refluxing the reaction for one to two hours, and TLC checked the process to make sure it was completed. By keeping at ambient temperature, the reaction combination, it was cooled. Following splitting, a solid mass was filtered and provided a water wash. Synthesized compounds' physical characterization data has been provided in Table 1.

2.3. Pharmacological activity

2.3.1. Anticancer Activity[13]: MTT assay was employed on human breast cancer celles-MCF-7 to determine the potential anticancer activity of novel 1,2.4-triazole connected quinoline derivatives. This invitro assay quantifies cell viability and proliferation, providing a measure of the compound's impact. The experiment involved testing six different concentrations of each compound, repeated three time for reliability. Doxorubicin was used as a standard for comparison, and the resulting cytotoxic data is summarized in Table-2.

2.3.2. Anthelmintic Activity[14]:

By observing how they influenced earthworms, the anthelmintic effectiveness of a variety of triazole-linked quinoline derivatives (3a–3j) was investigated. The standard anthelminthic prescription drugs, albendazole, and each test chemical have been given in various amounts (0.1%, 0.2%, and 0.5% w/v, dissolved in normal saline with very little DMSO) to six earthworms that were roughly the same size. Figures 5 and 6 illustrate the average times for complete paralysis and death, and this were recorded throughout the study. Table 3 provided details regarding these endpoints for both the tested and standard drugs.

2.3.3. Antibacterial Activity[15].

The entire series of newly synthesized triazole linked quinoline derivatives was screened for antibacterial properties against a panel of Agar diffusion assay detects Gram-positive (Bacillus subtilis, Staphylococcus aureus)

and Gram-negative (Escherichia coli, Klebsiella pneumoniae) the microorganism. The test substances were dissolved in methanol and bare minimum DMSO (1-2 ml) to attain an identical concentration of 100 μg/ml. Streptomycin, a frequently employed antibiotic, has been produced in a same volume. The diameter of the growth inhibition zones (in mm) was computed to measure the percentage of antibacterial activity during incubation; outcomes can be found in Table 4.

2.3.4. Molecular Docking Studies:

It was employed the in silico molecular modeling tool AutoDock Vina [16] to investigate potential drug candidate against Pokeweed Antiviral Protein (PAP). A receptor grid, crucial for identifying the protein's active site and preparing it for ligand docking, was generated to represent the receptor's shape and properties through various fields for precise ligand pose scoring. Ten compounds, designed using ACD/ChemSketch and prepared in MDL Molfile format after 3D optimization, were converted to PDBQT format with Open Babel. By deleting distant water molecules, inserting hydrogen atoms and missing residues, and minimizing energy, the MGL tool was utilized to enhanced the three-dimensional structure of Epidermal Growth Factor Receptor tyrosine kinase (PBD ID: 1M17), that was extracted from the protein data bank. The resulting binding energies and key interacting amino acids for the dataset ligands are presented in Table 5, providing insights for future drug design.

3. RESULTS AND DISCUSSION

3.1. Spectral data:

Compound - 3a:4-{(quinolin-3yl)methylidene)amino}-5-phenyl-4H-1,2,4-triazole-3-thiol.

IR (ν cm^{-1}): SH stretching at 3664cm-1 in triazole ring; Aromatic stretching (C-H) at 3003cm-1. Aliphatic(-C-H-) stretching at 2934, 2896cm-1; -C=N- stretching at 1603cm-1; Aromatic -C=CH- stretching at 1523cm-1; stretching at 132 and 1297cm-1 indicates due to C=C and C-C groups respectively. **^{1}H-NMR (DMSO) $\delta\delta$ ppm:** ν=10.276 singlet(1H) due to SH-triazole; singlet at 9.876ppm due Imine (CH=N, 1H) proton; Aromatic singlet proton at 8.209ppm(1H); 7.978ppm singlet proton due to Aromatic-H; doublet protns(2H) at 7.823-7.810ppm indicates aromatic-H; triplet(3H) aromatic-H at 7.634-7.601ppm; aromatic doublet protons(2H) at 7.554-7.482ppm; and triplet aromatic-H(2H) at 7.423-7.401ppm respectively. **^{13}C-NMR (DMSO) $\delta\delta$ ppm:** 158.54, 154.65, 145.62, 143.42, 143.76, 139.72, 136.32, 133.18, 130.43, 129.56, 126.03, 125.87, 125.86, 122.76, 120.76, 119.43, 56.12, 38.65. **MS m/z**(%) 331.09(M^+); 332.04(M^++1, 100).

Compound-3b:4-{(8-methylquinolin-3yl) methylidene) amino}-5-phenyl-4H -1,2,4-triazole-3-thiol.

IR (ν cm^{-1}): Triazole-SH stretching at 3654cm-1; stretching at 3087cm-1 due to aromatic-CH; Aliphatic(-CH-) stretching around 2993, 2848, 2784cm-1; Imine -C=N stretching at 1610cm-1; Stretching(-C=CH) in aromatic at 1519cm-1; Aromatic-C=C and C-C stretching at 1365, 1284cm-1 respectively. **^{1}H-NMR (DMSO) $\delta\delta$ ppm:** singlet protons of triazole-SH(1H) at 10.834ppm; Imine proton at 9.802ppm with singlet(1H); aromatic singlet protons(1H) at 8.532ppm; aromatic proton with singlet(1H) at 7.934ppm; doublet protons(2H) around 7.782-7.683ppm; aromatic doublet protons(2H) at 7.541-7.521ppm; triplet aromatic-H(3H) at 7.389-7.302ppm; triplet aromatic-H(1H) at 6.853ppm; singlet methyl protons ($ArCH_3$, 3H) at 2.002ppm respectively. **^{13}C-NMR (DMSO) $\delta\delta$ ppm:** 154.34, 147.32, 143.65, 140.12, 138.57, 136.44, 135.12, 133.87, 130.18, 128.59, 125.21, 124.56, 123.14, 120.54, 118.32, 116.56, 59.21, 39.52. **MS m/z**(%) 345.10(M+); 346.02(M^++1, 100).

Compound - 3c: 4-{(2-chloro-8-methylquinolin-3yl) methylene) amino} -5-phenyl-4H-1, 2,4-triazole-3-thiol.

IR (ν cm^{-1}): Stretching of triazole-SH at 3493cm-1; Aromatic-CH stretching at 3126 and 3126cm-1; aliphatic-CH stretching around 2938, 2742cm-1; Imine –C=N- stretching at 1609cm-1; Aromatic-C=CH stretching at 1477cm0-1; C=C and C-C stretching at 1268, 1161cm-1; aromatic-Cl stretching at 821cm-1 respectively. **^{1}H-NMR (DMSO) $\delta\delta$ ppm:** singlet proton at 10.894ppm due to triazole-SH(1H); aromatic singlet proton(1H) at 8.882ppm; singlet imine proton(1H) at 8.682ppm; aromatic singlet(1H) at 8.527ppm; triplet aromatic protons(1H) around 8.325ppm; aromatic doublet protons(2H) between at 7.934-7.863ppm; Aromatic doublet hydrogen's(2H) at 7.758-7.721ppm; triplet protons at 7.635-7.612ppm due to aromatic-H(3H); singlet methyl protons(3H, Ar-CH_3) at 2.687ppm respectively. **^{13}C-NMR (DMSO) $\delta\delta$ ppm:** 148.08, 147.92, 145.98, 144.23, 140.21, 138.65, 133.33, 131.28, 129.56, 128.11, 126.45, 125.91, 124.07, 122.32, 118.67, 115.43, 110.03, 56.43, 20.05**. MS m/z**(%) 379.07(M^+); 380.20(M^++1, 100); 381.03(M^++2, 30).

Compound - 3d: 4-{(2-chloro-8-methoxyquinolin-3yl)methylidene)amino}-5-phenyl-4H-1,2,4-triazole-3-thiol.
IR(νcm^{-1}): Triazole-SH stretching absorption at 3386cm-1; aromatic-CH stretching at 3018cm-1; aliphatic stretching (-CH-) absorption at 2911, 2885, 2784cm-1; Stretching at 1613cm-1 due to Imine group(C=N); Aromatic-CH stretching at 1512cm-1; aromatic C=C and C-C stretching at 1358, 1285cm-1; Aromatic-Cl stretching at 745cm-1. **^{1}H-NMR (DMSO) $\delta\delta$ ppm:** Singlet proton at 10.874ppm due to troazole(SH, 1H); singlet proton(1H) at 9.799ppm due to the imine group; 9.799(s, 1H, CH=N *Str,* imine proton), singlet and doublet protons are showing chemical shift between 8.199-7.664ppm due to aromatic hydrogen's(5H); triplet aromatic protons(4H) at 7.510-7.493ppm; singlet at 3.799ppm as a methoxy hydrogen's(3H) respectively. **^{13}C-NMR (DMSO) $\delta\delta$ ppm:** 152.16, 145.18, 139.32, 137.33, 136.72, 135.12, 132.83, 130.32, 128.06, 126.34, 124.56, 123.54, 122.18, 120.34, 116.93, 114.22, 58.32, 39.54.
MS m/z(%): 3495.06(M); 496.21(M$^+$+1, 100%); 497.32(M$^+$+2, 30%).

Compound-3e:4-{(8-methoxyquinolin-3yl)methylidene)amino}-5-phenyl-4H-1,2,4-triazole-3-thiol.
IR (νcm^{-1}): Triazole-SH stretching at 3580cm-1; aromatic CH- stretching absorption at 3081cm-1; CH- stretching in aliphatic absortion at 2915, 2845cm-1; Imine stretching at 1611cm-1; stretching absorption at 1475cm-1 due to -C=H group; stretching absorption at 1263 and 1166cm-1 due to -C=C-, -C-C- groups. **^{1}H-NMR (DMSO) $\delta\delta$ ppm:** singlet proton(1H) at 11.584ppm due to triazole-SH; Imine proton(1H) at 9.803ppm as a singlet; singlet aromatic protons(2H) at 8.194-8.093ppm; triplet protons(3H) at 7.998-7.982 due to aromatic-H; doublet protons of aromatic-H(4H) at between 7.702-7.692ppm; aromatic triplet proton(1H) at 7.545-7.540ppm; singlet methoxy protons(3H) at 3.800ppm. **^{13}C-NMR (DMSO) $\delta\delta$ ppm:** 158.54, 154.54, 143.76, 141.21, 138.54, 134.87, 133.12, 130.43, 127.43, 125.02, 123.34, 121.43, 120.43, 119.43, 118.54, 115.76, 57.87, 36.4. **MS m/z(%):** 361.21(M); 362.32(M$^+$+1,100%).

Compound-3f:4-{(2-chloro-6-bromoquinolin-3yl)methylidene)amino}-5-phenyl-4H-1,2,4 -triazole-3-thiol.
IR (νcm^{-1}): Stretching at 3643cm-1 due Triazole-SH; Aromatic-CH stretching at 3062cm-1; Aliphatic-CH stretching at 2987, 2865 and 2765cm-1 respectively; Imine-N=CH stretching at 1620cm-1; Aromatic absorption at 1523cm-1 and -C=C stretching at 1334cm-1; stretching at (C-C) at 1283cm-1; Chlorine(Ar-Cl) and bromine(Ar-Br) stretching at 798 and 668cm-1. **^{1}H-NMR (DMSO) $\delta\delta$ ppm:** Triazole-SH protons(singlet, 1H) at 10.986ppm; singlet triazole protons(1H) at 10.986ppm; singlet imine proton(CH-=N) at 9.698ppm; singlet, doublet and triplet aromatic protons(8H) between 8.209-7.321ppm respectively. **^{3}C-NMR (DMSO) $\delta\delta$ ppm:** 158.94, 148.96, 142.94, 140.12, 138.32, 136.23, 135.13, 132.17, 127.43, 125.32, 123.43, 122.34, 120.54, 118.45, 115.12, 113.54, 56.54. **MSm/z(%):** 442.95(M); 443.42(M$^+$+1, 100%); 444.14(M$^+$+2, 30%).

Compound-3g:4-{(2-chloro-quinolin-3yl)methylidene)amino}-5-phenyl-4H-1,2,4-triazole -3-thiol.
IR(νcm^{-1}): Triazole-SH stretching absorption at 3603cm-1; Aromatic-CH stretching at 3093cm-1; aliphatic-CH stretching at 2963, 2876cm-1; Imine-CH=N stretching at 1623cm-1; Aromatic-CH- and C=C stretching at 1487 and 1262cm-1; the C-C stretching at 1194cm-1; the Ar-Cl stretching at 803cm-1. **^{1}H-NMR (DMSO) $\delta\delta$ ppm:** singlet trazole-SH(1H) proton at 10.684ppm; singlet imine proton (CH=N) at 8.894ppm; all aromatic-H with singlet, doublet and triplet proton(10H) at 8.420-7.321ppm respectively. **^{13}C-NMR (DMSO) $\delta\delta$ ppm:** 150.25, 148.15, 145.67, 142.18, 140.98, 137.23, 136.02, 134.35, 131.78, 129.43, 125.04, 123.15, 121.55 119.43, 116.23, 115.33, 56.22. **MSm/z(%):** 365.05(M); 366.32(M$^+$+1, 100%); 367.45(M$^+$+2, 30%).

Compound-3h:4-{(2-chloro-8-methylquinolin-3yl)methylidene)amino}-5-phenyl-4H-1,2, 4-triazole-3-thiol.
IR (ν cm^{-1}): stretching at 3582cm-1 due to Triazole-SH; aromatic stretching(CH-) at 3102cm-1; stretching at 2978, 2856 and 2789cm-1 due to aliphatic-CH; Imine(CH-=N) stretching at 1619cm-1; Stretching at 1497cm-1 due to Ar-CH; aromatic-C=C and C-C stretching at 156 and 1182cm-1; stretching at 798cm-1 due to Ar-Cl. **^{1}H-NMR (DMSO) $\delta\delta$ ppm:** Triazole-SH protons(1H, singlet) at 10.904ppm; singlet imine(CH=N) proton(1H) at 8.923ppm; all aromatic protons(12H) with singlet, doublet and triplet at 8.323- 7.218ppm; singlet methyl proton(3H) at 2.126ppm. **^{13}C-NMR (DMSO) $\delta\delta$ ppm:** 153.92, 150.21, 148.76, 144.12, 141.62, 139.34, 137.12, 135.87, 130.26, 128.43, 124.19, 122.19, 120.43 118.78, 115.03, 113.73, 58.39, 29.17. **MS m/z(100%):** 379.07(M); 380.14(M$^+$+1, 100%); 381.71(M$^+$+2, 30%).

Compound - 3i: 4-{(2-chloro-5-methoxyquinolin-3yl)methylidene) amino}-5-phenyl-4H-1,2,4-triazole-3-thiol.
IR (ν cm^{-1}): Stretching at 3610cm-1 due to Triazole-SH; Aromatic-CH stretching at 3078cm-1; aliphatic-CH stretching at 2987, 2842 and 2791cm-1; imine stretching(-CH=N) at 1615cm-1; C=C- stretching at 1483cm-1; C=C, C-C stretching at 1245 and 1143cm-1; Aromatic-Cl stretching at 807cm-1. **^{1}H-NMR (DMSO) $\delta\delta$ ppm:** singlet triazole-SH(1H) at 10.827ppm; Singlet imine proton(1H) at 8.826ppm; aromatic protons(9H) at 8.287-7.301ppm; singlet methoxy proton(3H) at 3.682ppm. **^{13}C-NMR (DMSO) $\delta\delta$ ppm:** 155.32, 151.65, 150.54, 148.01, 144.51, 137.65, 135.26, 133.18, 131.54, 127.71, 123.65, 121.83, 121.65 119.04, 116.45, 115.76, 59.54, 36.03. MS m/z(%): 395.06(M^+); 396.34(M^++1, 100); 397.04(M^++2, 30).

Compound-3j:4-{(2-fluoroquinolin-3yl)methylidene)amino}-5-phenyl-4H-1,2,4-triazole-3-thiol.
IR (νcm^{-1}): stretching at 3592cm-1 due to triazole-SH; Aromatic-CH stretching at 3104cm-1,
Stretching at 2984, 2882cm-1 due to aliphatic; Imine-CH=N stretching at 1473cm-1; C=C and C-C stretching at 1272 and 1186cm-1; stretching at 803cm-1 due to Ar-F. **^{1}H-NMR (DMSO) $\delta\delta$ ppm:** singlet proton(1H) at 10.784ppm due to triazole-SH; singlet imine (1H, CH=N) proton at 8.761ppm; singlet, doublet and triplet protons(10H) due to aromatic-H respectively. **^{13}C-NMR (DMSO) $\delta\delta$ ppm:** 153.86, 146.94, 147.74, 145.23, 143.54, 140.32, 138.14, 135.73, 133.16, 130.43, 128.02, 125.54, 123.76, 120.54, 118.43, 116.34, 58.92. MS m/z(%): 349.08(M^+); 350.32(M^++1, 100); 352.64(M^++2, 30).

3.2. Pharmacological Activity.

3.2.1. Anticancer activity. The MTT assay was employed to screen the synthesized triazole linked unfamiliar Quinoline Derivatives-I(3a-3j) for anticancer activity employing the MCF-7 cell line with the objective to predict the cell viability with IC50 values. In accordance with the results provided in Table 2, MCF-7 cell lines were susceptible to the investigated compounds, exhibiting IC50 values that varied from 20.02±0.013 µg to 58.99±0.381 µg against the MCF7 cell line. With effective activity revealed by their IC50 values of **23.46±0.001, 20.02±0.013, and 25.76±0.016 µg**, compounds 3b, 3f, and 3j were the most potent derivatives. on the other hand, the remaining compounds displayed moderate potency.

3.2.2. Anthelmintic activity. Table 3 describes an actual anthelmintic activity final result, and Figure 4 presents the activity comparison. The data indicated that all of the medications under study had good-to-great activity. Excellent activity has been shown by compounds **3b, 3c, 3h,** and 3j among the substances screened; these compounds were equivalently comparable to the standard treatment albendazole.

3.2.3. Antibacterial Activity:

In the present investigation, the triazole-linked novel Quinoline Derivatives-I(3a-3j) were synthesized and tested for their antibacterial efficacy against gram-positive and gram-negative bacterial strains, as well as using the agar cup plate diffusion method. While compared to the standard, compounds 3a, 3b, 3d, 3h, and 3j illustrated strong antimicrobial activity against Gram-negative bacteria (Escherichia coli, Klebsiella pneumonia) and Bacillus subtilis and Staphylococcus aureus.

3.3. Molecular Docking Studies:

Auto Dock Vina was utilized to molecularly dock the dataset compounds against the target protein's active site in order to examine any potential interactions between proteins and ligands. The binding energies for each one of the ten docked ligands, which ranged from -10.8 to -9.1 Kcal/mol, are provided in Table 4, together with the numbers of the interacting amino acid residues. Additionally, it has been demonstrated that compounds 3f, 3b, and 3j each produced one single hydrogen bond with the amino acids. ASP:831, LYS:721, MET:742, LEU:764, LEU:820, VAL:702, ALA:719, PHE:699, and MET:742.

International Journal of Environmental Sciences
ISSN: 2229-7359
Vol. 11 No. 16s, 2025
https://www.theaspd.com/ijes.php

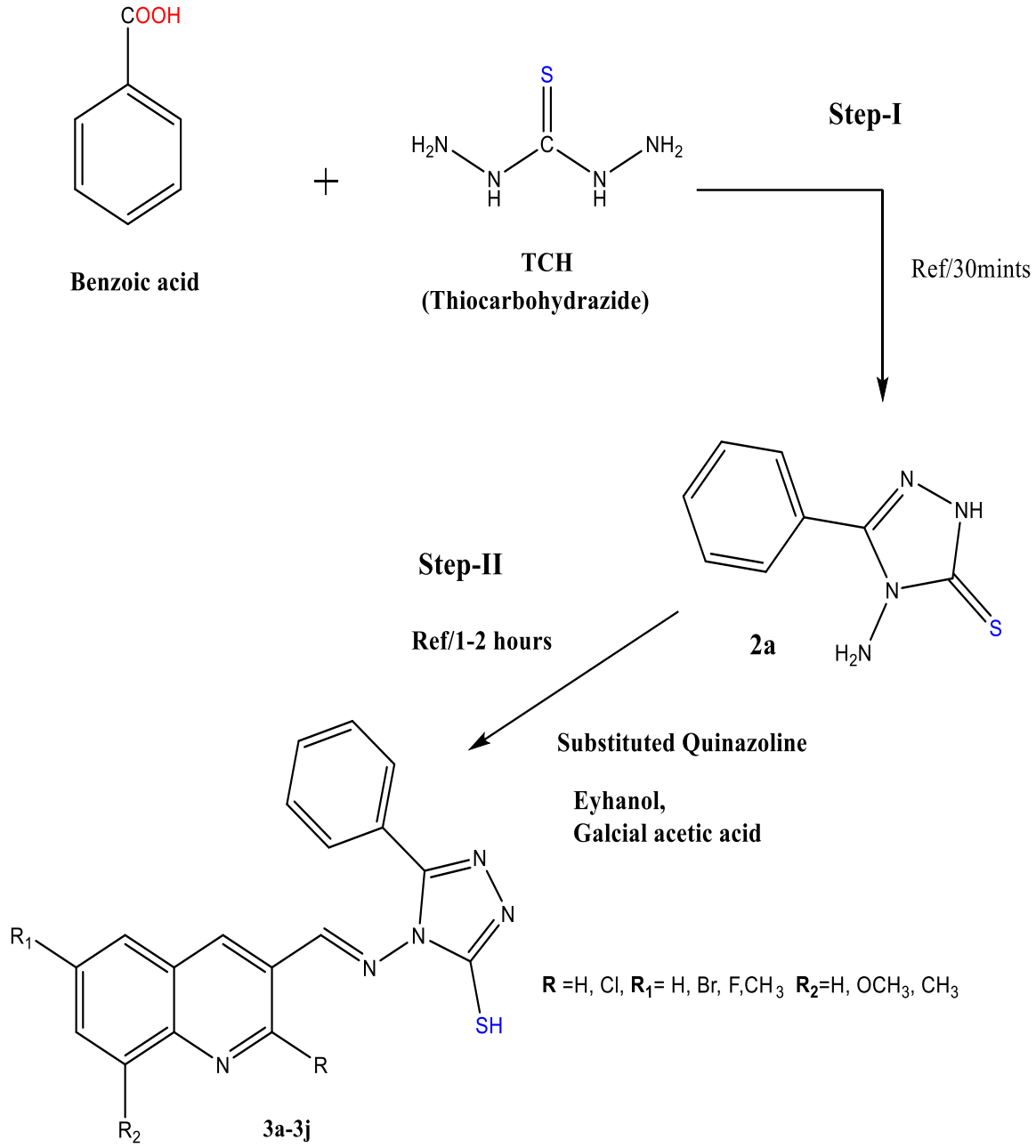

Fig.No.1. Schematic representation of synthesis of triazole linked novel Quinazoline derivatives 1-(3a-3j).

Table 1. Physical Data of triazole linked novel Quinazoline derivatives I-(3a-3j)

S.NO	R	R_1	R_2	Mol. For	Mol. Wt.	M.P(^{O}C)	%Yield
I-3a	H	H	H	$C_{18}H_{13}N_5S$	331.09	201-203	78
I-3b	H	H	CH_3	$C_{19}H_{15}N_5S$	345.10	187-189	83
I-3c	H	Cl	CH_3	$C_{19}H_{14}N_5ClS$	379.07	241-243	81
I-3d	H	Cl	OCH_3	$C_{19}H_{14}N_5OS$	395.06	169-171	78
I-3e	H	H	OCH_3	$C_{19}H_{15}N_5OS$	361.10	157-159	75
I-3f	Cl	Br	H	$C_{18}H_{11}N_5BrClS$	442.96	143-145	86
I-3g	Cl	H	H	$C_{18}H_{12}N_5ClS$	365.05	195-197	80
I-3h	Cl	CH_3	H	$C_{19}H_{14}N_5ClS$	379.07	211-213	77
I-3i	Cl	OCH_3	H	$C_{19}H_{14}N_5OClS$	395.06	219-221	85
I-3j	H	F	H	$C_{18}H_{12}N_5FS$	349.08	231-233	80

International Journal of Environmental Sciences
ISSN: 2229-7359
Vol. 11 No. 16s, 2025
https://www.theaspd.com/ijes.php

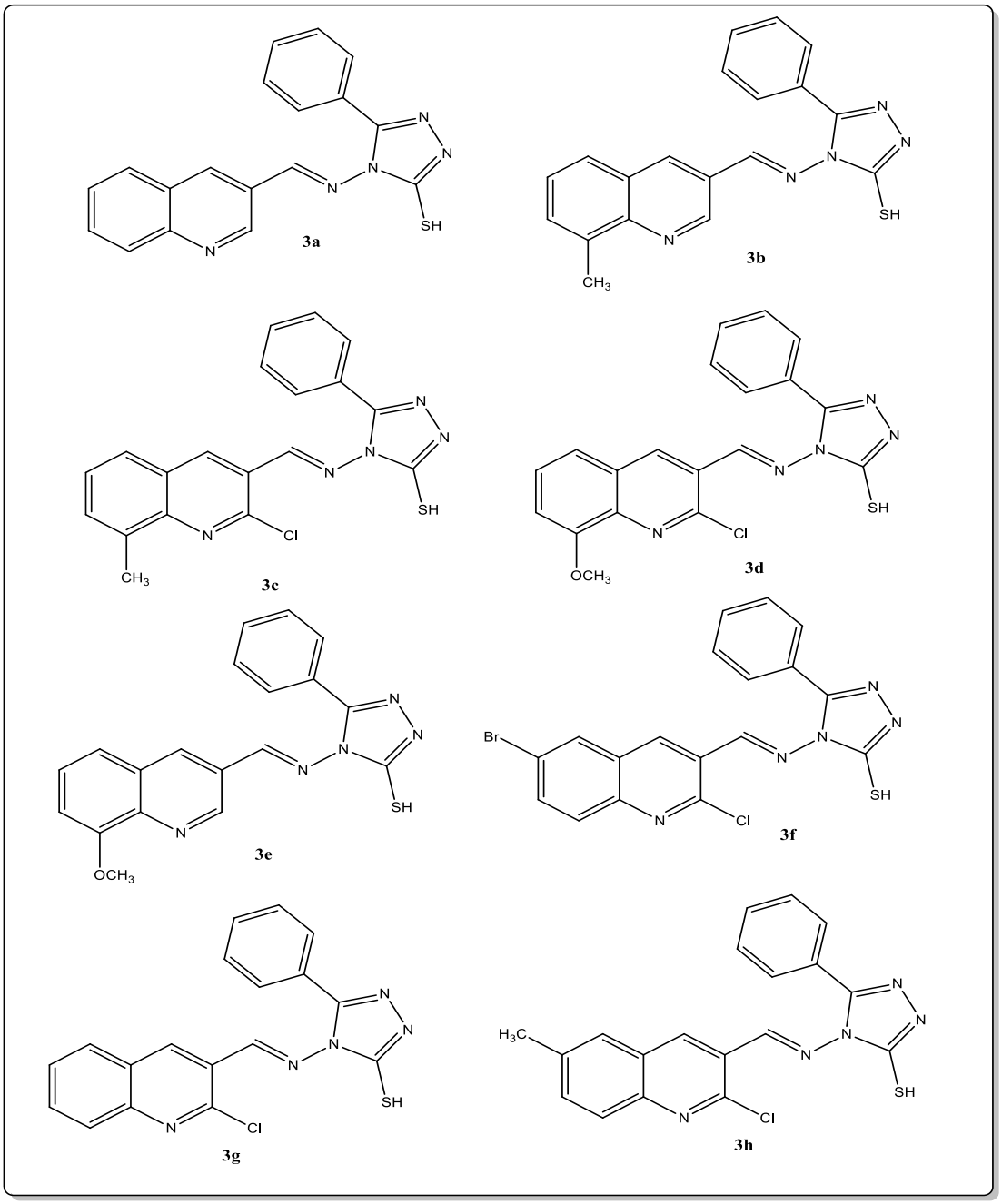

Fig.No.2 The triazole fused novel Quinazoline derivatives 1(3a-3j) (Scheme-I)

Table.2: Anticancer activity with IC_{50} values of Novel triazole linked Quinoline Derivatives I-(3a-3j)

Sample Name	MCF -7[(IC_{50} (µg)]
I-3a	53.15±0.324
I-3b**	**23.46±0.001**
I-3d	41.87±0.403
I-3f**	**20.02±0.013**
I-3h	58.99±0.381
I-3j**	**25.76±0.016**
Doxorubicin	**11.48±0.001**

International Journal of Environmental Sciences
ISSN: 2229-7359
Vol. 11 No. 16s, 2025
https://www.theaspd.com/ijes.php

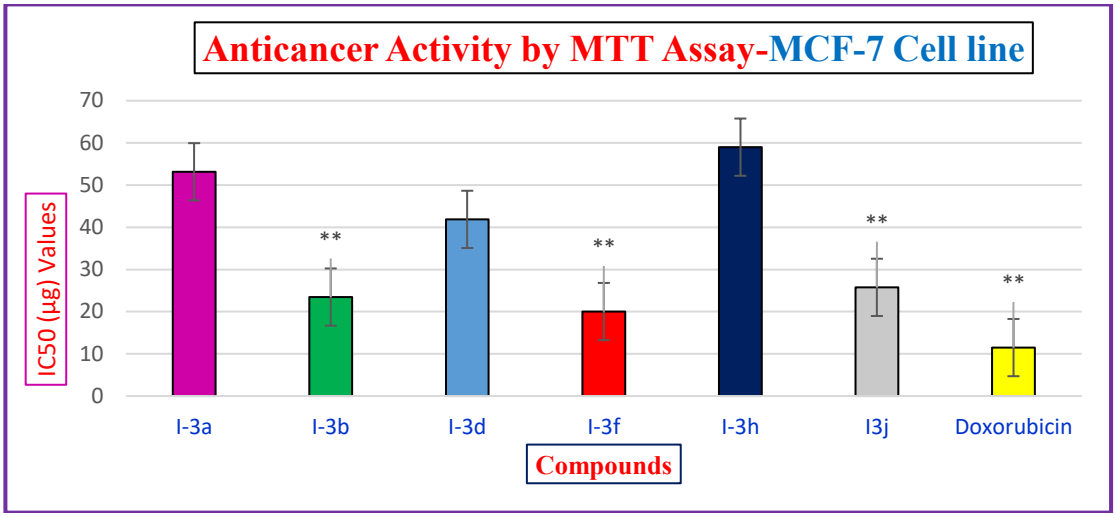

Figure 3: Graphical representation of anticancer activity by MTT- IC_{50} (Mean ± S.E.M). n=6.

Table.No.3. Anthelmintic activity of triazole linked novel Quinoline Derivatives (3a-3j)

S.No.	Name	Time in minutes					
		For paralysis % Concentration			For death % Concentration		
	Concentration	0.1	0.2	0.5	0.1	0.2	0.5
	Control	-	-	-	-	-	-
	Albendazole	17	12	8	40	32	23
1	I-3a	33	26	20	58	50	37
2	I-3b	19	15	12	46	37	25
3	I-3c	18	13	10	41	34	27
4	I-3d	36	29	23	67	56	44
5	I-3e	35	27	23	60	56	45
6	I-3f	36	24	22	57	48	44
7	I-3g	32	23	20	63	51	44
8	I-3h	19	13	11	42	35	26
9	I-3i	28	21	16	66	57	48
10	I-3j	17	15	12	44	36	29

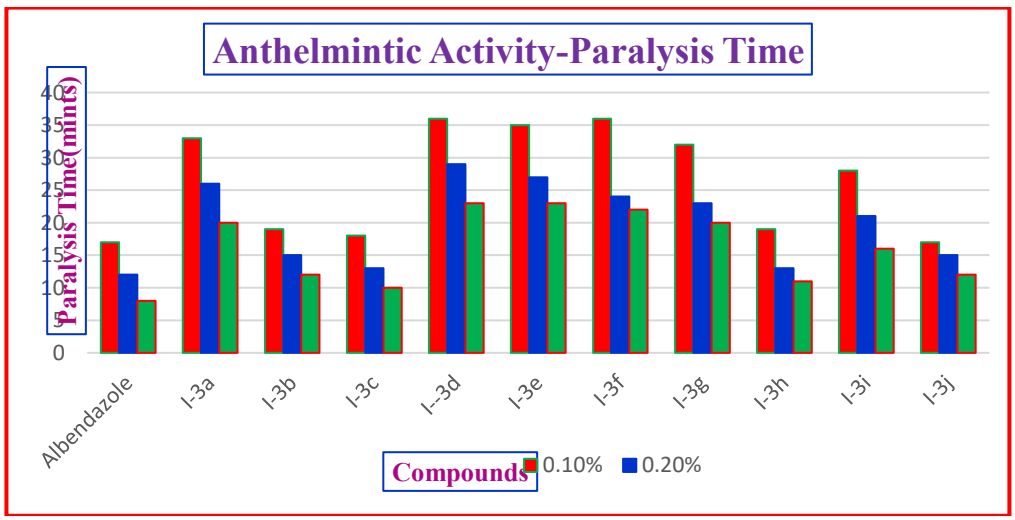

Figure 4: Anthelmintic activity of novel Quinoline derivatives linked to triazoles-I(3a-3j)–Paralysis time (min) is artistically displayed.

International Journal of Environmental Sciences
ISSN: 2229-7359
Vol. 11 No. 16s, 2025
https://www.theaspd.com/ijes.php

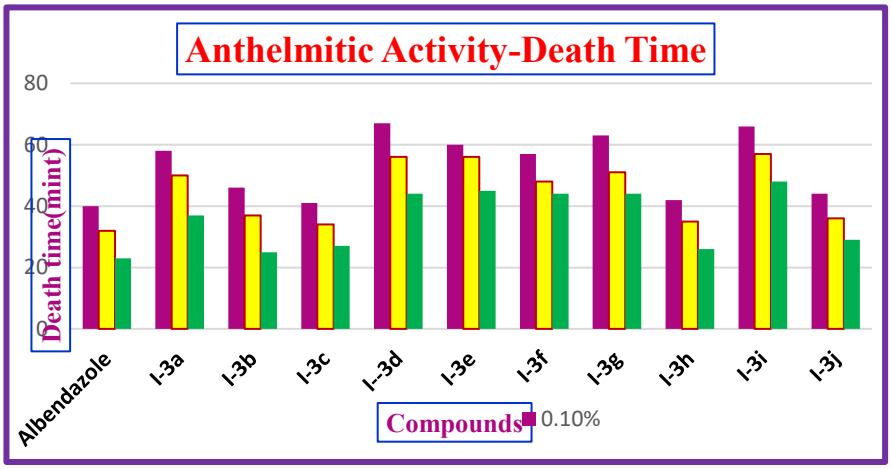

Figure 5: Anthelmintic responses of novel Quinoline derivatives linked to triazoles-I(3a-3j)–Death time (min) is schematically represented.

Table 4: Antibacterial activity of triazole linked novel Quinoline Derivatives (3a-3j) Death time (min)-Zone of inhibition (in mm).

Compounds	Zone of Inhibition (in mm)			
	Bacillus subtilis	*Staphylococcus aureus*	*Escherichia coli*	*Klebsiella pneumonia*
Streptomycin	33	31	30	32
I-3a	26	24	10	23
I-3b	23	26	23	12
I-3c	16	9	12	10
I-3d	24	25	10	23
I-3e	11	13	10	15
I-3f	10	9	12	16
I-3g	9	18	10	12
I-3h	25	24	13	23
I-3i	10	9	14	10
I-3j	26	23	9	25

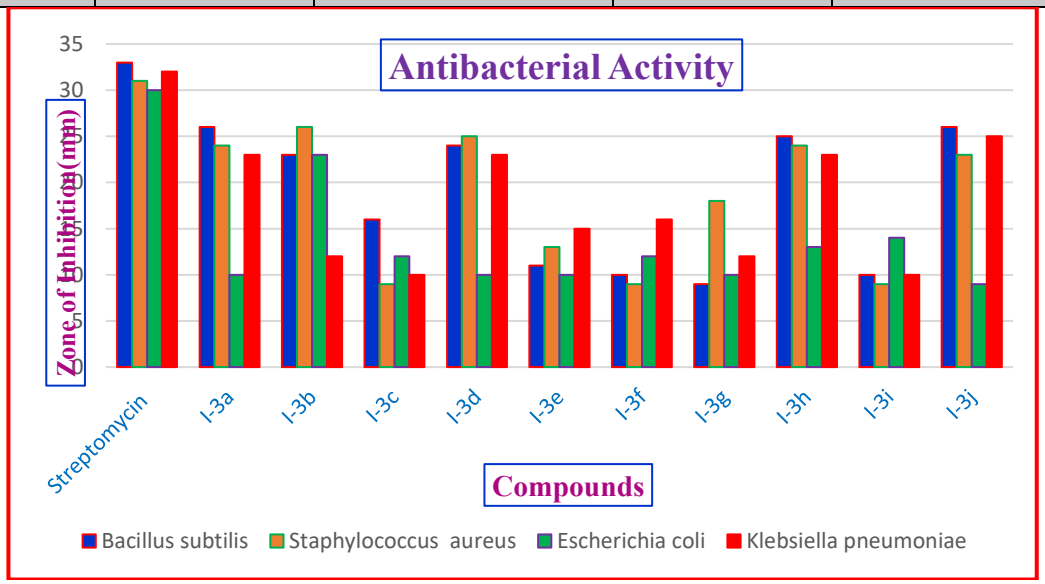

Figure 6. Graphical representation of antibacterial activity of triazole linked novel Quinoline Derivatives-I(3a-3j).

International Journal of Environmental Sciences
ISSN: 2229-7359
Vol. 11 No. 16s, 2025
https://www.theaspd.com/ijes.php

Table-5: *Insilco* EGFR inhibition of triazole linked novel Quinoline Derivatives-I(3a-3j)-Binding Energy.

Compound No	Binding Energy (Kcal/mol)	No of H-Bonds	Interacting amino acids	H-bond lengths (Å)
I-3f	-10.8	Nil	PHE-699,VAL-702,ALA-719,LYS-721, MET-742,LEU-764,LEU:-820	Nil
I-3b	-10.7	Nil	PHE-699,VAL-702,ALA-719,LYS-721,MET-742,LEU-820,ASP:-831	Nil
I-3j	-10.6	Nil	VAL-702,ALA-719,LYS-721, LEU-764,LEU-820	Nil
I-3c	-10.5	Nil	VAL-702, ALA-719, LYS-721, MET-742	Nil
I-3g	-10.4	Nil	VAL-702, LYS-721, MET-742, LEU-820	Nil
I-3d	-10.4	Nil	PHE-699,VAL-702,ALA-719, LYS-721,CYS-773,LEU:-820,ASP-831, ASN-818	Nil
I-3i	-9.3	Nil	PHE-699, ALA-719, MET-742, LEU-764,	Nil
I-3h	-9.1	Nil	PHE-699, VAL-702, ALA-719, LYS-721, MET-742	Nil

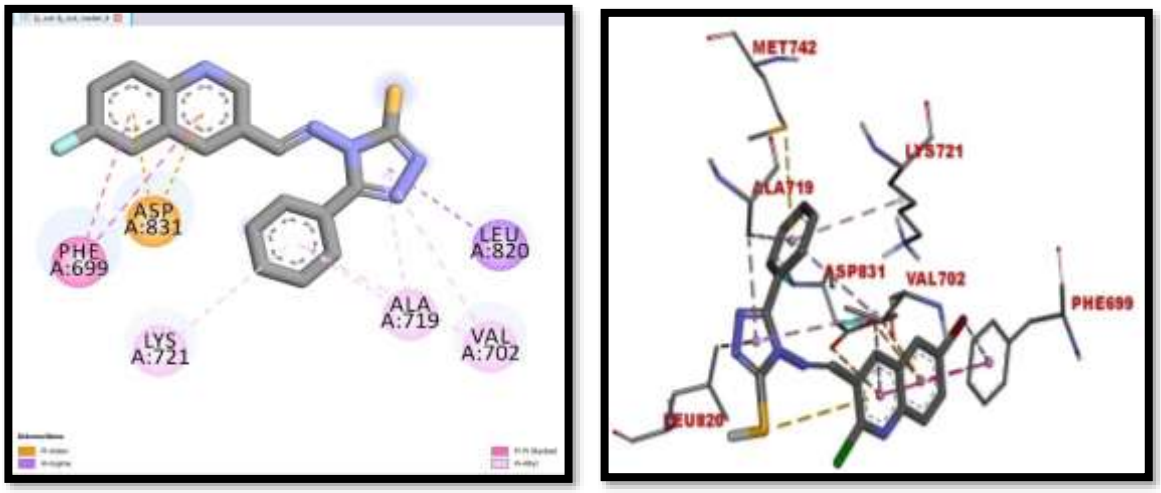

3b (Dock1-2d, Dock-2-3d)

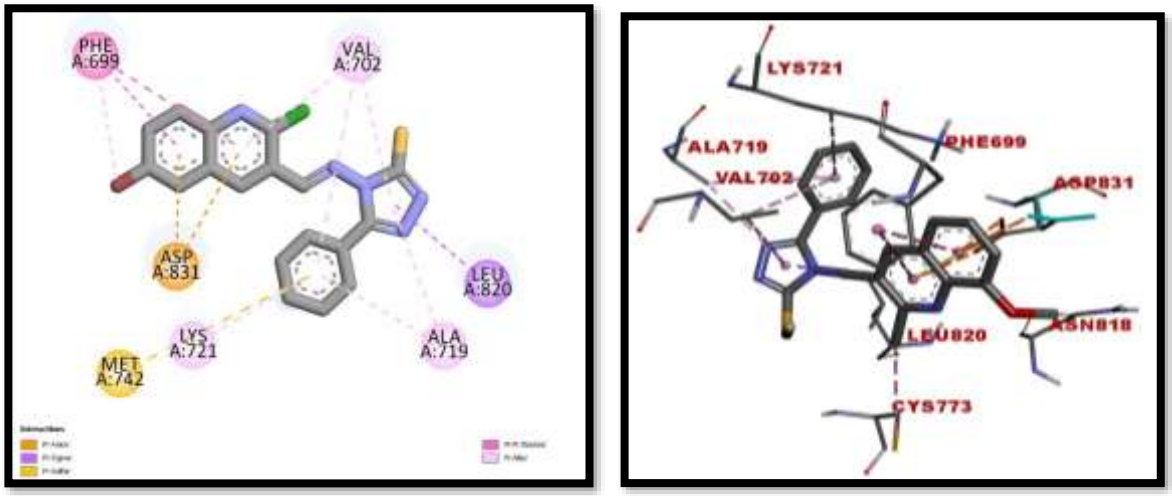

3d (Dock1-2d, Dock-2-3d)

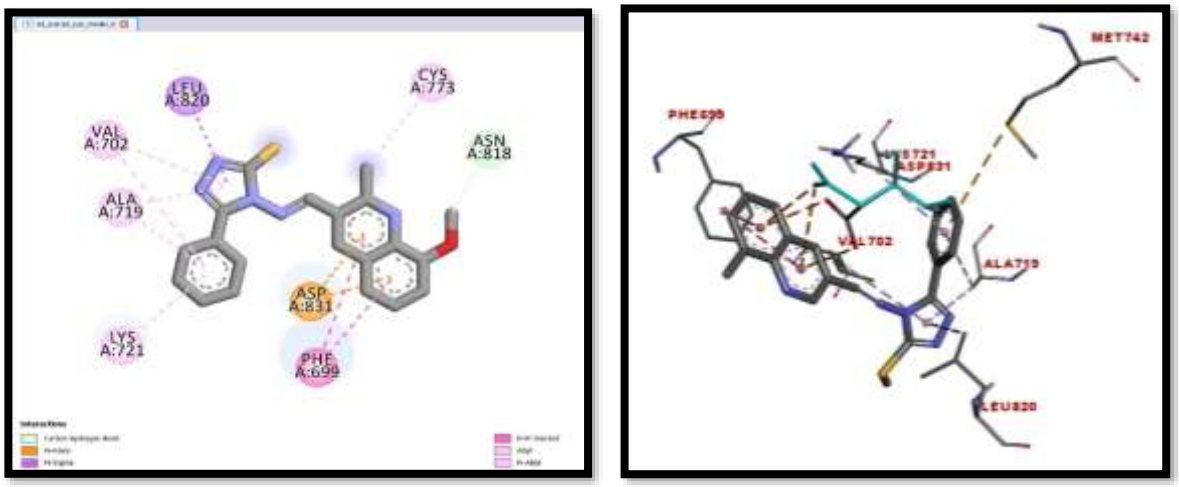

3f (Dock1-2d, Dock-2-3d)

Figure.No.7. Ligand and Protein Docking Pose (3b, 3d, and 3f) -dock-1 2D and dock-2 3D images.

4.CONCLUSION

Novel 1,2,4-triazole coupled quinoline derivatives (3a–3j) have been effectively produced in this study using excellent yields (75-86%), and their structures have been confirmed spectroscopically. Compounds 3f and 3j have been identified as potential discoveries following biological examination revealed that they have excellent silico binding scores and significant anticancer, antibacterial, and anthelmintic activities. The remaining substances displayed moderate activity, providing insight into the links between structure and activity for ongoing pharmaceutical formulation.

ACKNOWLEDGEMENTS

Authors would like acknowledge Department of Chemistry, Osmania University and Veeranari Chakali Ilamma Women's University, Hyderabad (Formerly University College for women) for providing research facilities.

Authors ORCID:

G. Sreelatha https://orcid.org/0009-0009-2768-5621.

Dr. P. Sateesh Kumar http://orcid.org/0000-0002-7523-1028

Dr. Aliya Begum https://orcid.org/0000-0001-6755-9413

CONFLICT OF INTEREST

The authors declare that they have no conflicts of interest with regard to the publication of this work.

References

1. Wan, Y.C., Fang, G.Q., Chen, H.J., Deng, X., and Tang, Z.L., Eur. J. Med. Chem., 2021, vol. 226, p. 113837. https://doi.org/10.1016/j.ejmech.2021.113837.
2. S. Abraham, B. Mallika, A. Reshma and R.M. Kassim, Case Rep Dent.,2019, 2521685 (2019); https://doi.org/10.1155/2019/25216852.
3. W.Y. Wang, W.Y. Wu, A.L. Li, Q.S. Liu, Y. Sun, W. Gu, Bioorg. Chem.,109, 104705 (2021); https://doi.org/10.1016/j.bioorg.2021.10470514.
4. K.D. Katariya, S.R. Shah and D. Reddy, Bioorg. Chem., 94, 103406 (2020). https://doi.org/10.1016/j.bioorg.2019.10340615.
5. H.A.A. Ezelarab, H.A. Hassan, G.E.A. Abuo-Rahma and S.H. Abbas,J. Iran. Chem. Soc., 20, 683 (2023); https://doi.org/10.1007/s13738-022-02704-716.
6. A. Asbat, F. Saleem, S. Najm, J. Iqbal, M.A. Syed, S. Ahmad, S. Hanif,M. Azeem. J. Mol. Struct., 1264, 133234 (2022); https://doi.org/10.1016/j.molstruc.2022.133234.
7. Pavelyev, R.S., Bondar, O.V., Nguyen, T.N.T., Ziganshina, A.A., Farroukh, M.A., Karwt, R., Alekbaeva, G.D., Pugachev, M.V., Yamaleeva, O.N., Balakin, K.V., and Shtyrlin, Y.G., Bioorg. Med. Chem., 2018, vol. 26, p. 5824. https://doi.org/10.1016/j.bmc.2018.10.031

8. S. Thakur, A. Jaryal and A. Bhalla, Results Chem., 7, 101350 (2024); https://doi.org/10.1016/j.rechem.2024.101350.
9. M. Badwelan, H. Muaddi, A. Ahmed, K.T. Lee and S.D. Tran, Curr.Oncol.,30, 3721 (2023); https://doi.org/10.3390/curroncol30040283.
10. Endoori, S., Gulipalli, K.C., Bodige, S., Ravula, P., and Seelam, N.V., *J. Heterocycl. Chem*., 2021, vol. 58, p. 1311. https://doi.org/10.1002/jhet.4259.
11. Marzaro, G., Coluccia, A., Ferrarese, A., Brun, P., Castagliuolo, I., Conconi, M.T., Regina, G.L., Bai, R., Silvestri. R., Hamel, E., and Chilin, A., J. Med. Chem., 2014, vol. 57, p. 4598. https://doi.org/10.1021/jm500034j
12. C. Boulechfar, H. Ferkous, A. Delimi, A. Djedouani, A. Kahlouche, A.Boublia, A.S. Darwish, T. Lemaoui, R. Verma and Y. Benguerba, Inorg.Chem. Commun., 150, 110451 (2023); https://doi.org/10.1016/j.inoche.2023.110451.
13. Quattrini, L., Gelardi, E.L.M., Coviello, V., Sartini, S., Ferraris, D.M., Mattia, M., Nakano, I., Garavaglia, S., and La Motta, C., J. Med. Chem., 2020, vol. 63, p. 4603. https://doi.org/10.1021/acs.jmedchem.9b01910.
14. Santoshi, S., Manchukonda, N.K., Suri, C., Sharma, M., Sridhar, B., Joseph, S., Lopus, M., Kantevari, S., Baitharu, I., and Naik, P.K., J. Comp.-Aided Mol. Design, 2015, vol. 29, p. 249. https://doi.org/10.1007/s10822-014-9820-5.
15. Z-F. Zeng, Q-P. Huang, J.-H. Cai, G-J. Zheng, Q-C. Huang, Z-L. Liu,Z-L. Chen and Y-H. Wei, Molecules, 26, 4028 (2021); https://doi.org/10.3390/molecules261340282474.
16. T.A. Yousef, A.G. Alhamzani, M.M. Abou-Krisha, G. Kanthimathi, M.S.Raghu, K.Y. Kumar, M.K. Prashanth and B.H. Jeon, Heliyon, 8, e13460(2023);.
https://doi.org/10.1016/j.heliyon.2023.e13460.
17. S. Hymavathi, Ameena Husain, N. Swathi, P. Sateesh Kumar, B. Anupama, Alia Begum. 2024. Asian Journal of Chemistry, Vol. 36, No. 12 (2024), 2801-2808. https://doi.org/10.14233/ajchem.2024.32630